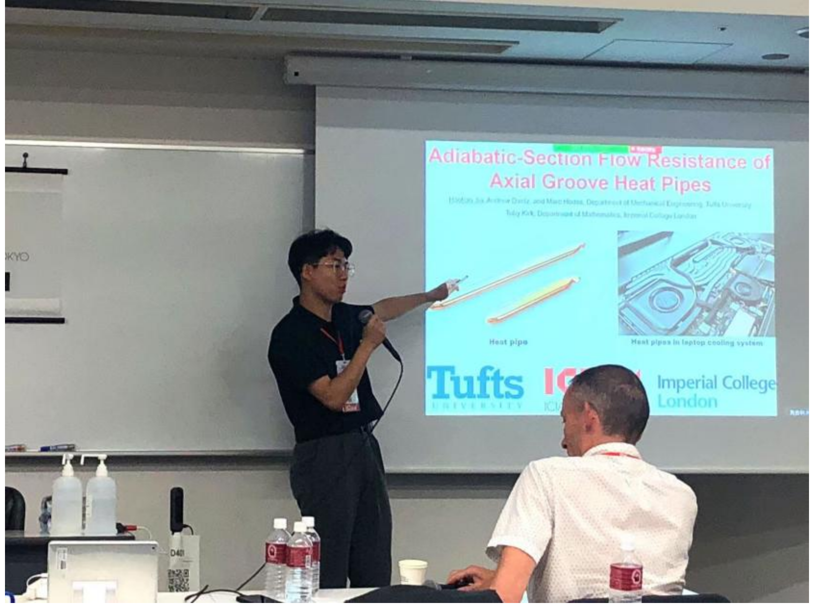

Haotian Jia, Department of Mechanical Engineering,
Tufts University

Mechanical Engineering PhD specializing in fluid mechanics & heat transfer, with extensive experience in design of experiments, testing & lab equipment, data acquisition, and precise thermal & fluid measurements.

Internal Flow Modeling of Heat Pipe

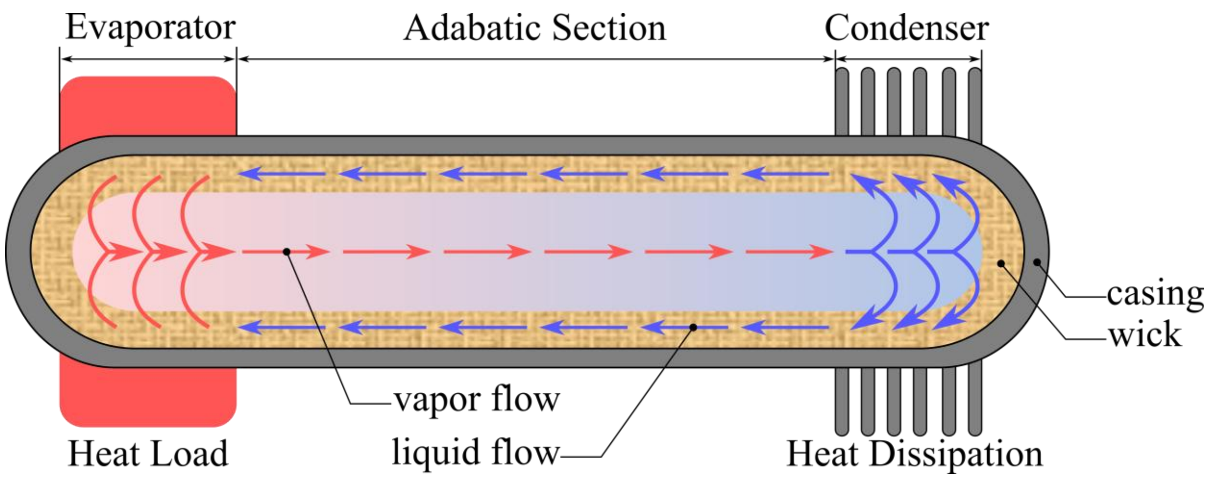

Schematic of heat pipe

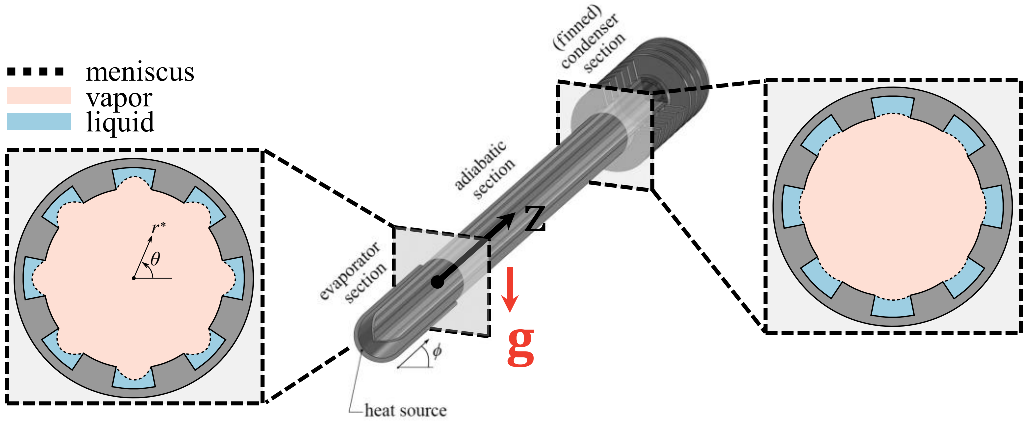

Schematic of Axial-grooved Heat Pipe

- heat pipes are highly effective thermal conductors. Their effective thermal conductivity can approach 100 kW/(m·K) for long heat pipes, in comparison with approximately 0.4 kW/(m·K) for copper.
- A heat pipe is made up of a casing (envelope), a wick structure, and a small amount of liquid. Heat is transferred into the heat pipe, causing the liquid to evaporate into vapor then travels along the pipe and condenses back into liquid at the condenser section in a continuous flow loop.
- Has 3 major wick types: sintered metal, screen mesh, and grooved.

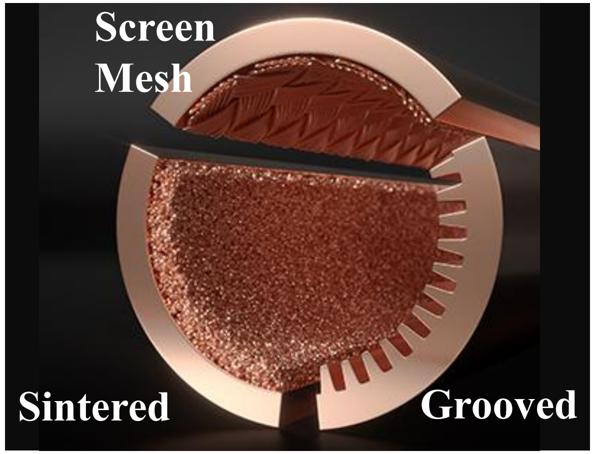

Wick types

- When the capillary pressure is not sufficient to pump the liquid back to the evaporator, the capillary limit is encountered, thus causes the dry out of the wick at evaporator.

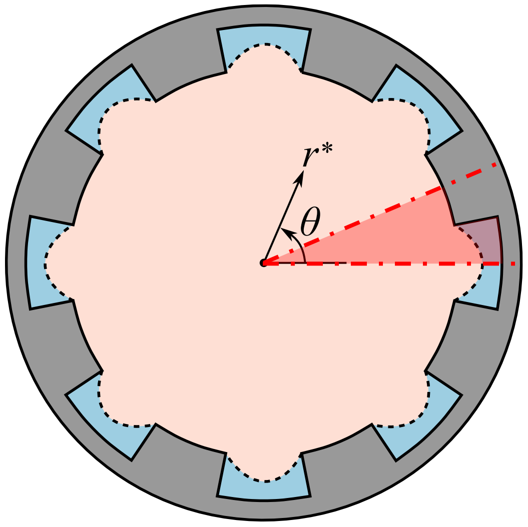

Problem domain

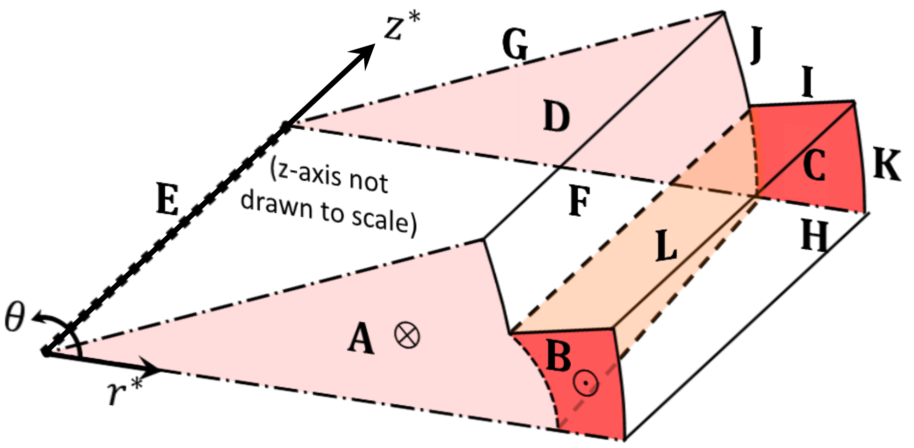

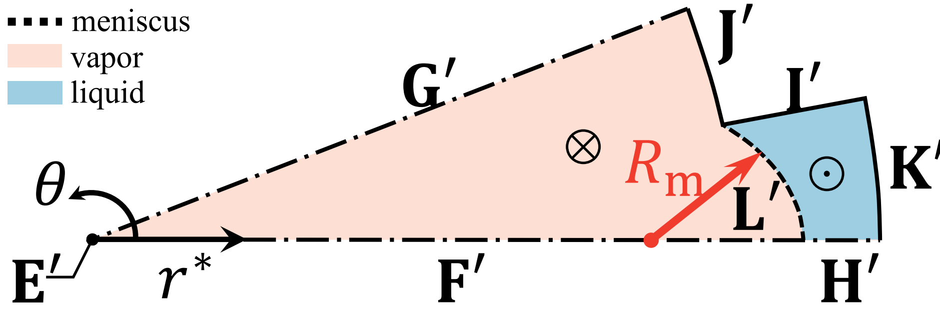

Complementary problem domain

- Continuity equation $\nabla^* \cdot \mathbf{v}_i^* = 0$
- Navier-Stokes equation $\rho_i \mathbf{v}_i^* \cdot \nabla^* \mathbf{v}_i^* = -\nabla^* p_i^* + \mu_i \nabla^{*2} \mathbf{v}_i^* + \rho_i \mathbf{g}$
- The stream-wise mass flowrate of liquid equal to vapor $\rho_{\mathrm{v}} Q_{\mathrm{v}}^* = \rho_{\mathrm{l}} Q_{\mathrm{l}}^*$

$$\frac{1}{r}\frac{\partial}{\partial r}\left(r\frac{\partial V_{z,\mathrm{v}}}{\partial r}\right)+\frac{1}{r^2}\frac{\partial}{\partial \theta}\left(\frac{\partial V_{z,\mathrm{v}}}{\partial \theta}\right)=1$$

$$\frac{1}{r}\frac{\partial}{\partial r}\left(r\frac{1}{\tilde{\mu}}\frac{\partial V_{z,\mathrm{l}}}{\partial r}\right)+\frac{1}{r^2}\frac{\partial}{\partial \theta}\left(\frac{1}{\tilde{\mu}}\frac{\partial V_{z,\mathrm{l}}}{\partial \theta}\right)=\tilde{\xi}$$

Table of boundary conditions along meniscus in cases A - C.

case	vapor in evaporator	vapor in adiabatic	vapor in condenser	liquid in evaporator	liquid in adiabatic	liquid in condenser
A	no slip	no slip	no slip	no slip	no slip	no slip
B	no slip	no slip	no slip	const. shear	const. shear	const. shear
C_0	no slip	this study, $O\left(\epsilon^0, \theta_{\mathrm{m}}^0\right)$	no slip	no slip	this study, $O\left(\epsilon^0, \theta_{\mathrm{m}}^0\right)$	no slip
C	no slip	this study, $O\left(\epsilon^0\right)$	no slip	no slip	this study, $O\left(\epsilon^0\right)$	no slip

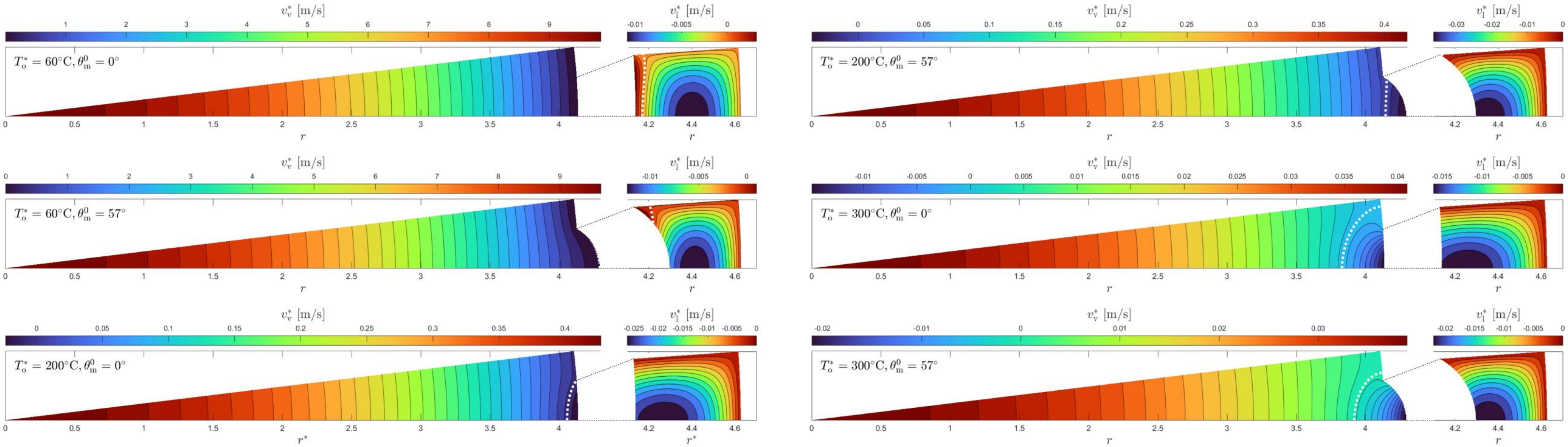

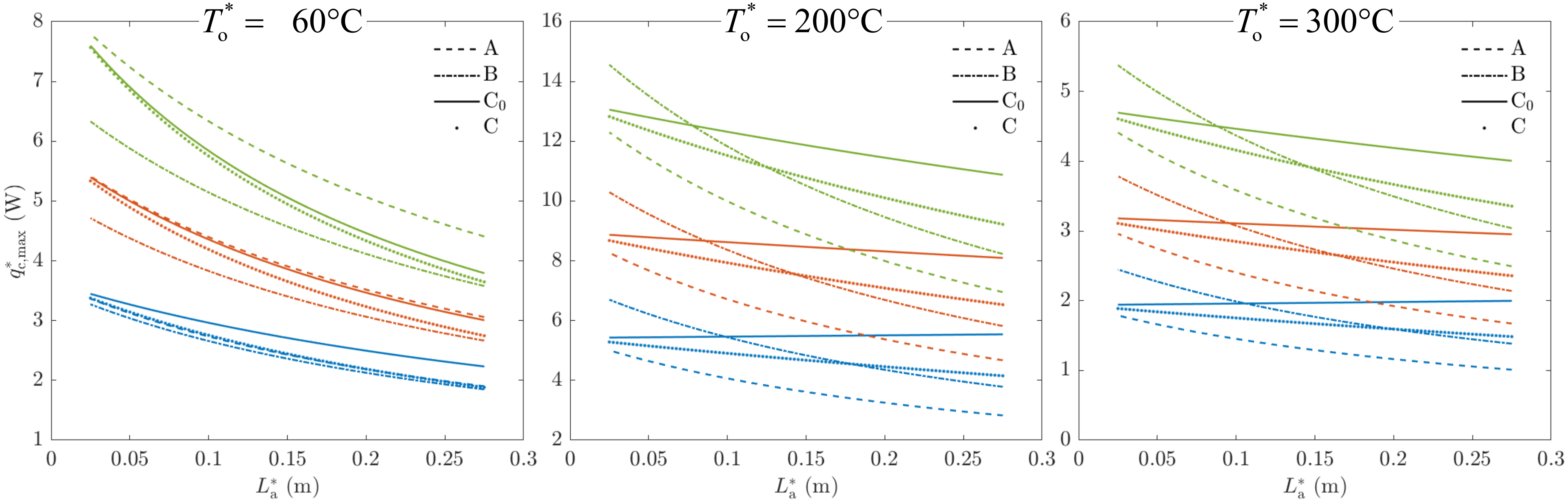

Capillary limit vs. adiabatic section length in 0.3 m-long AGHP with $L_e^* = L_c^*$, R_g^* = 1.18 mm, 1.20mm, and 1.22 mm.

Permeability Measurement of Aerogel, Supercritical Condition

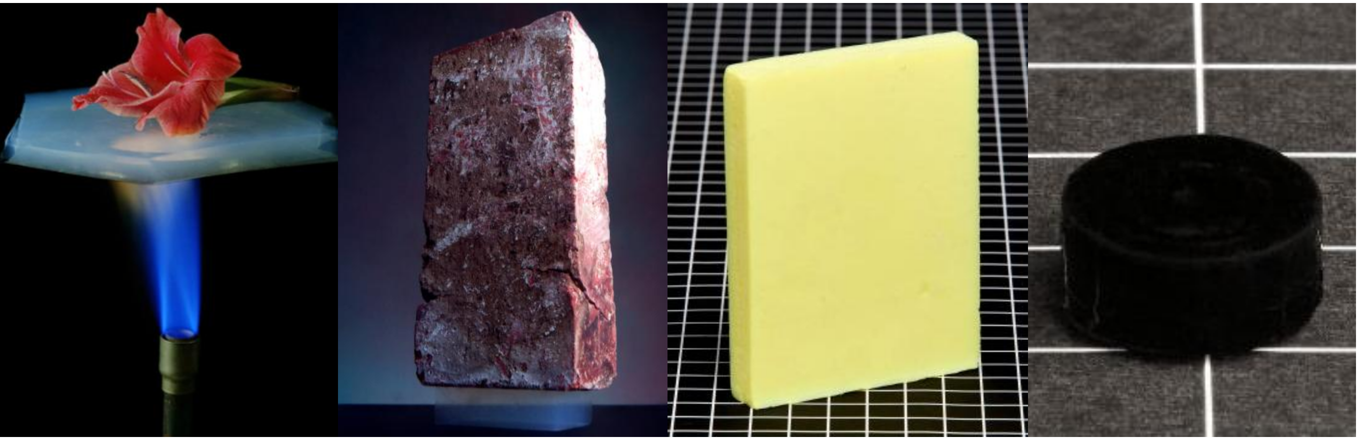

Aerogels, nanoporous, ultralight material that exhibits remarkable thermal insulation, soundproofing, or energy-absorbing properties.

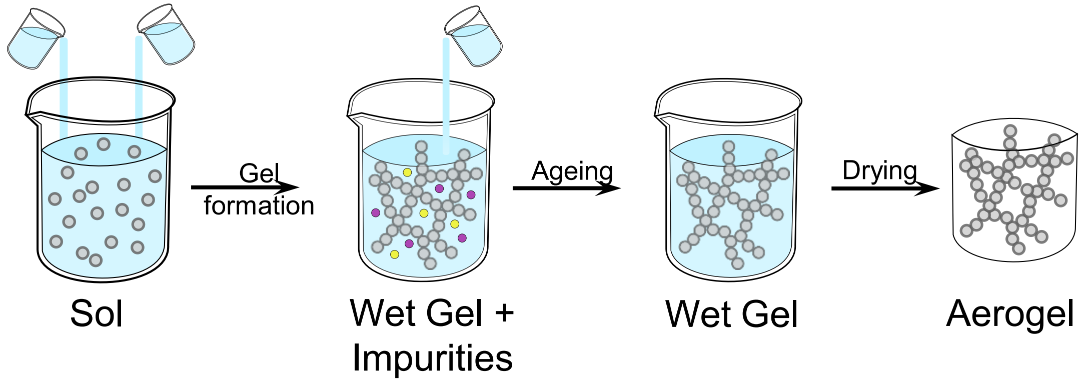

Aerogel manufacturing process

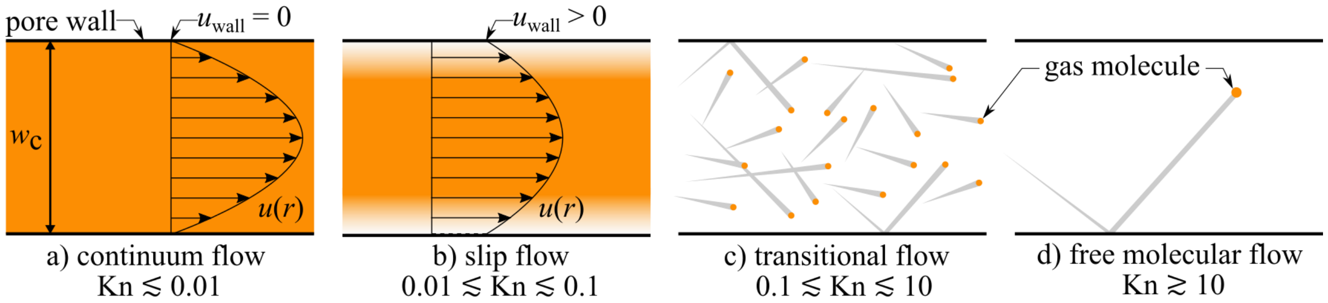

Flow regime at Kn range

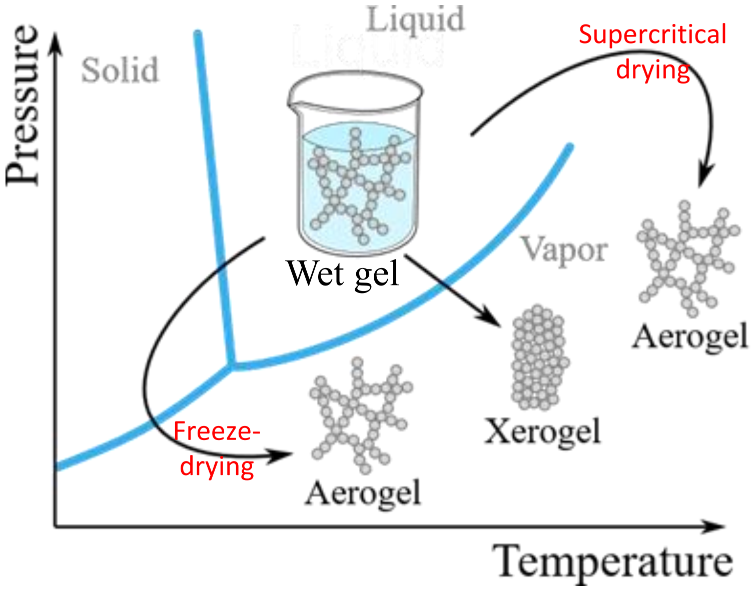

Concentrical pore fluid p-T phase diagram

Direct Method

- Permeability is determined by 1-D Darcy's equation $K = \mu Q H / (A_c \Delta p)$,
  where Q, H, A_c, and Δp are flowrate, thickness, cross-sectional area, and pressure difference, respectively.

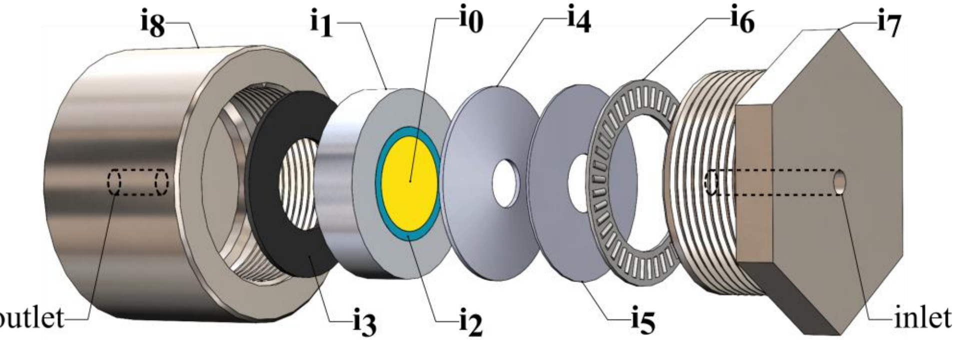

Direct method test section exploded view

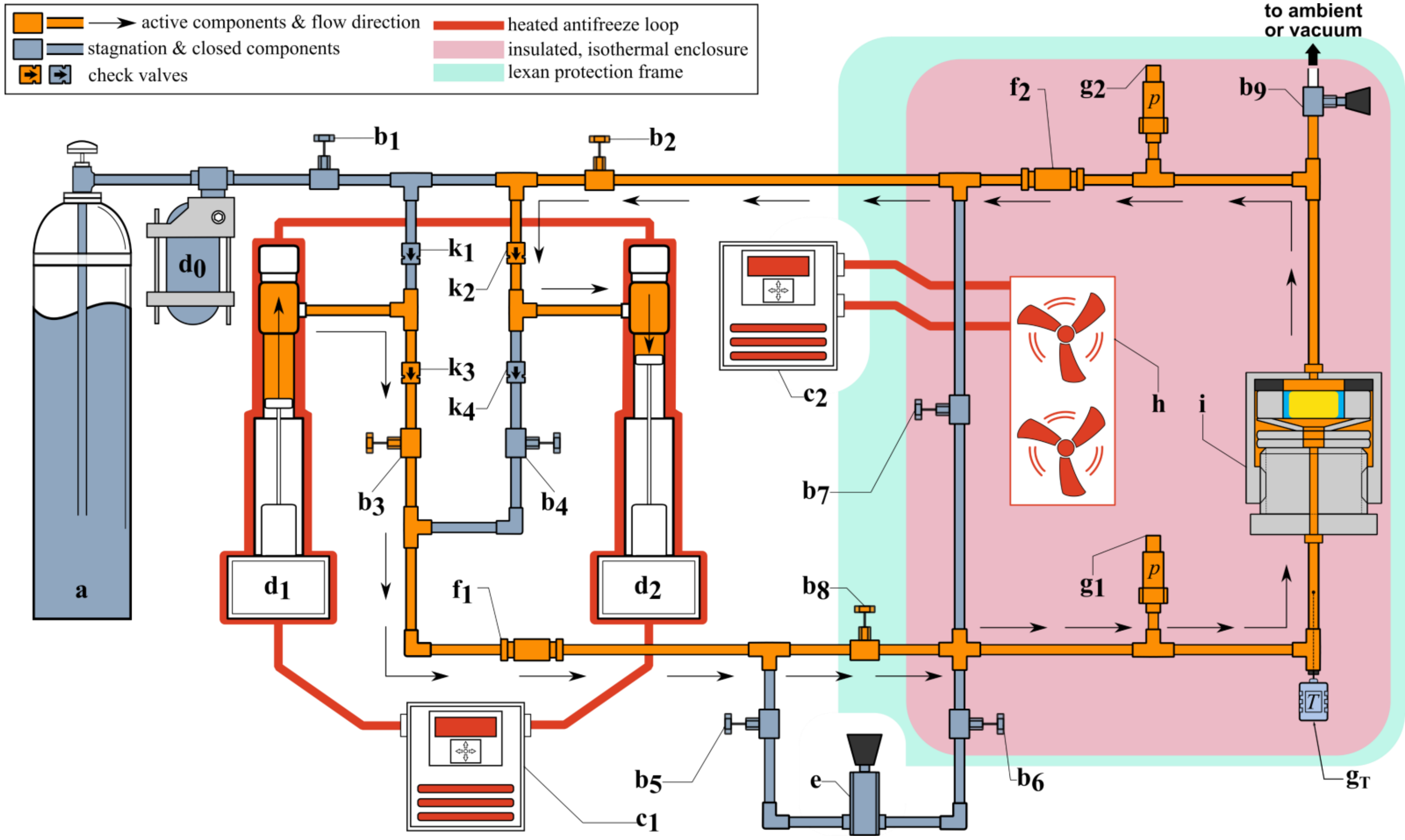

Direct method apparatus schematic

Inverse Method

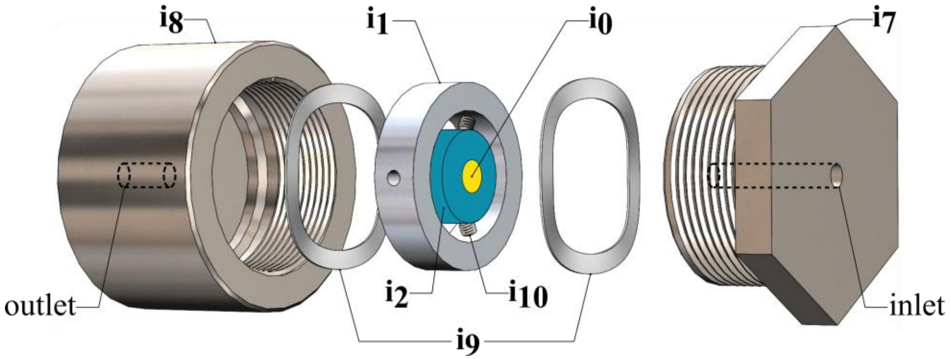

Inverse method test section exploded view

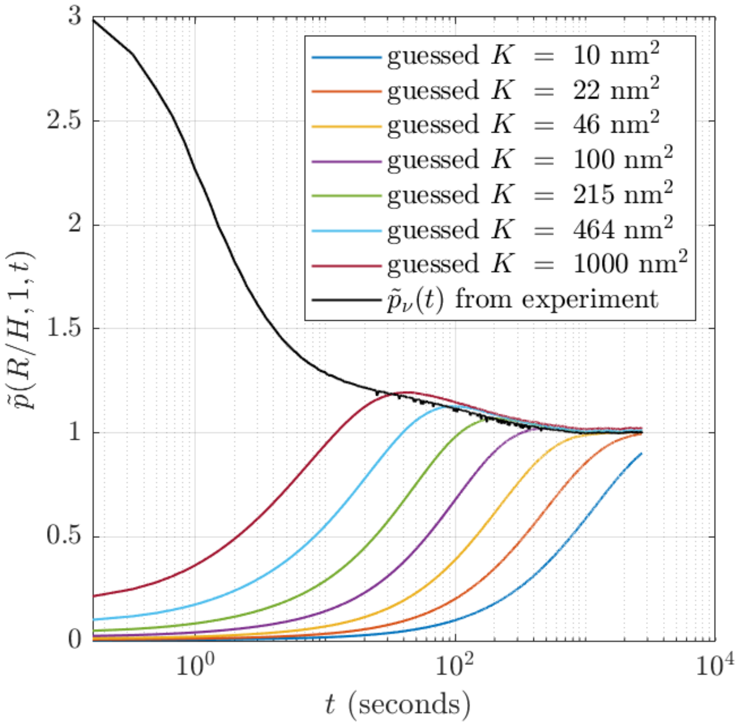

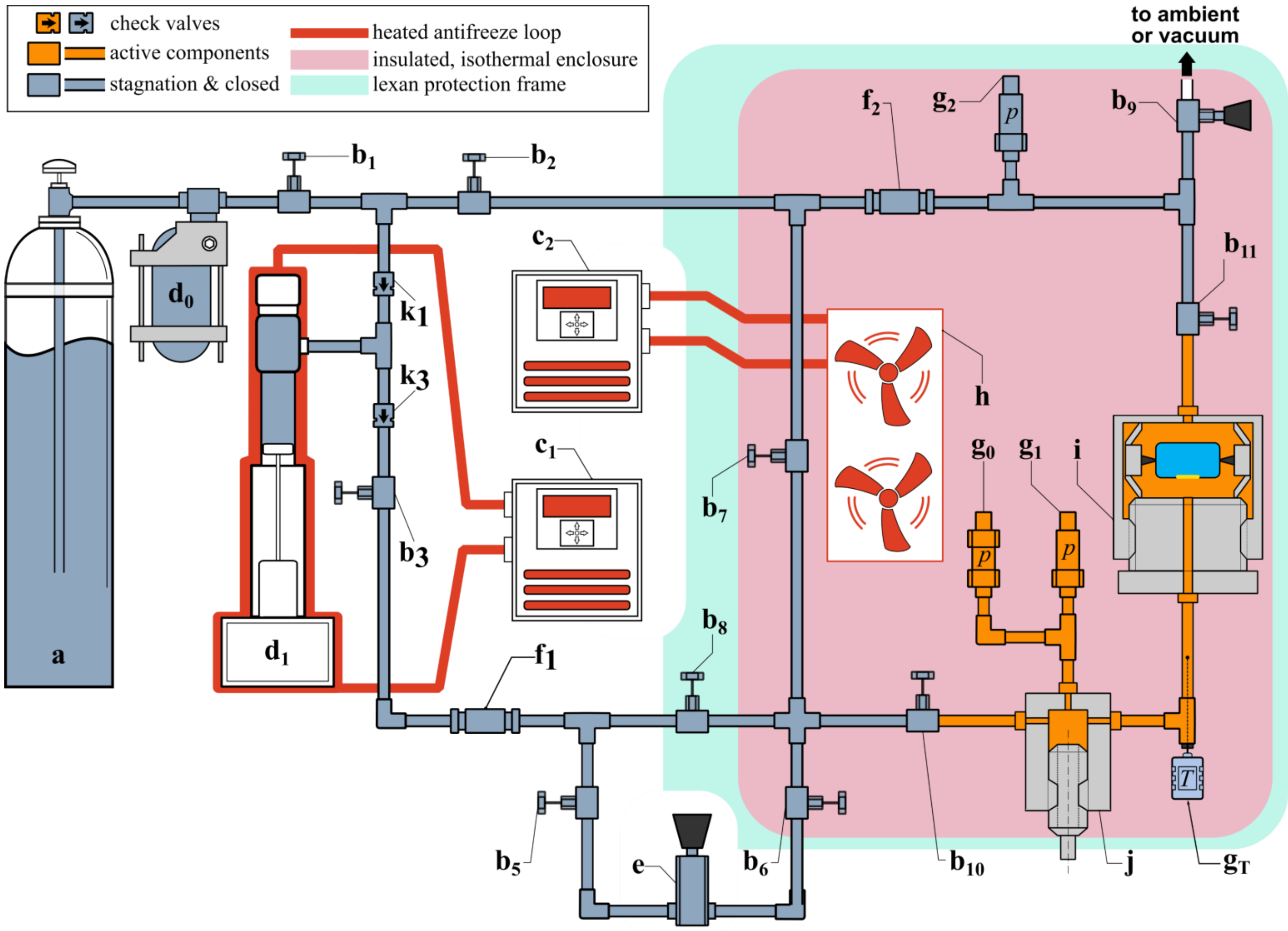

Inverse method apparatus schematic

Jet-impingement Enhanced Aerogel Freeze-drying

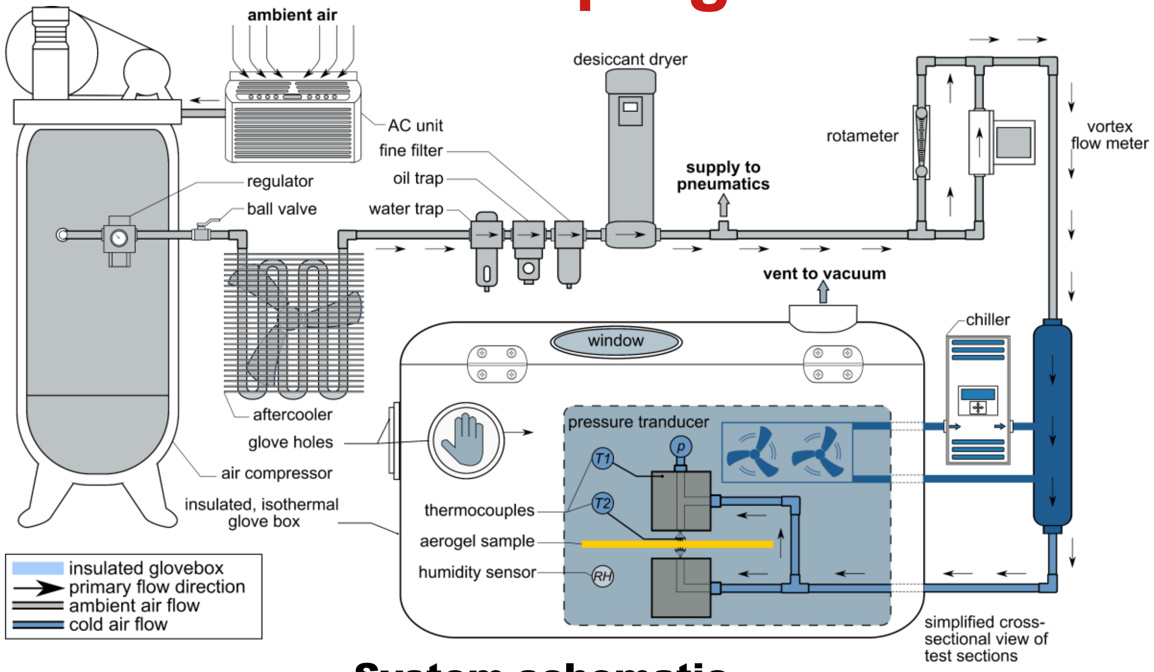

System schematic

System photo

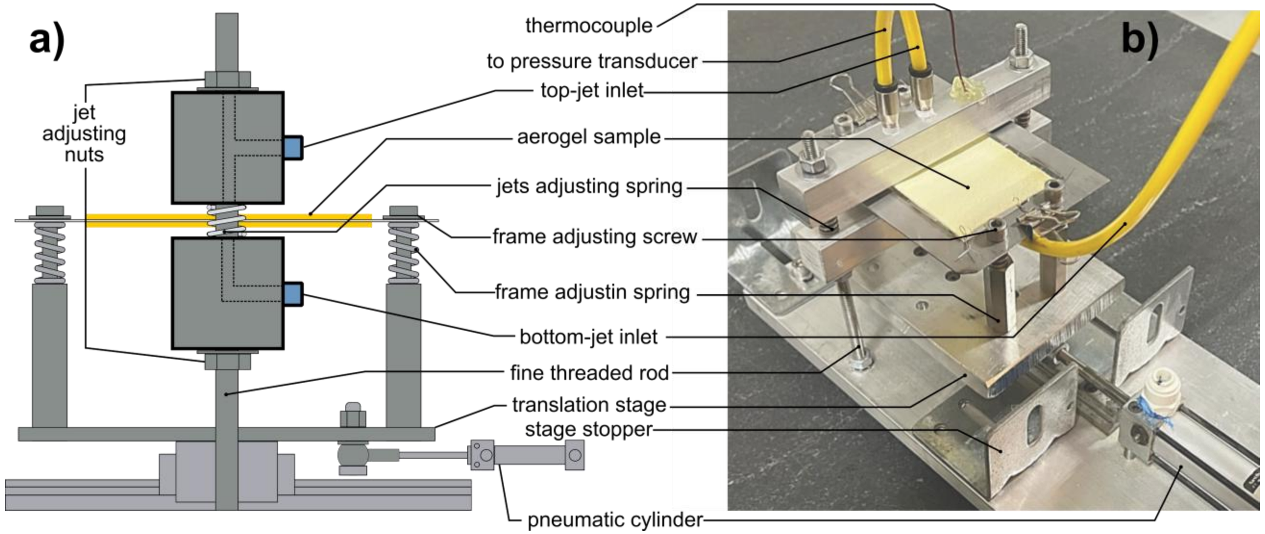

Test section schematic

NOKIA Bell Labs, Thermal Management COOP

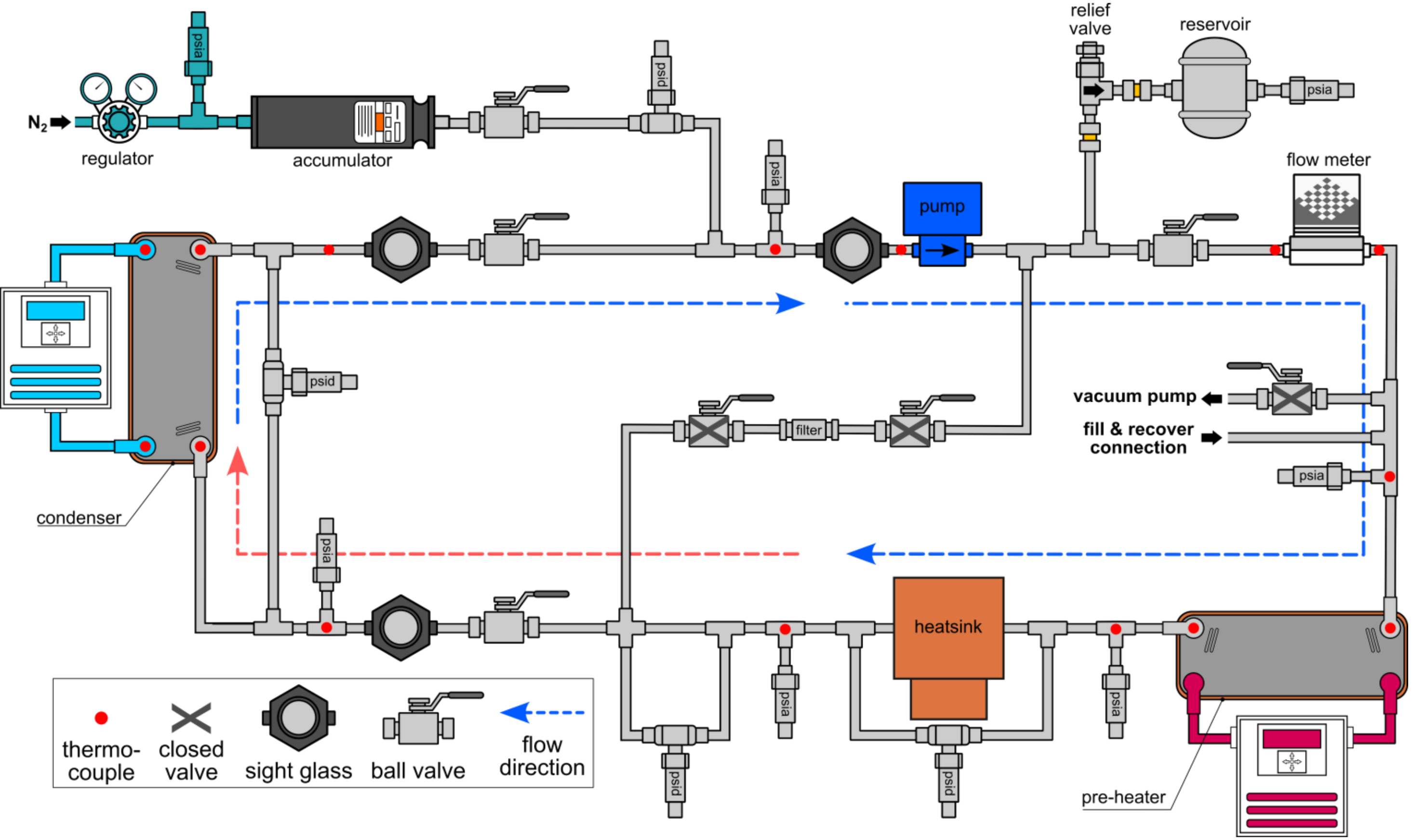

Pump loop schematic

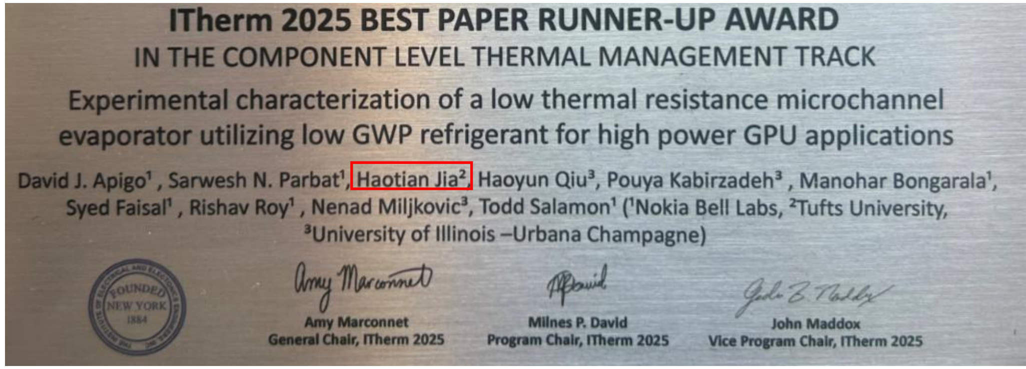

IEEE iTherm2025 Best Paper Runner-up Award

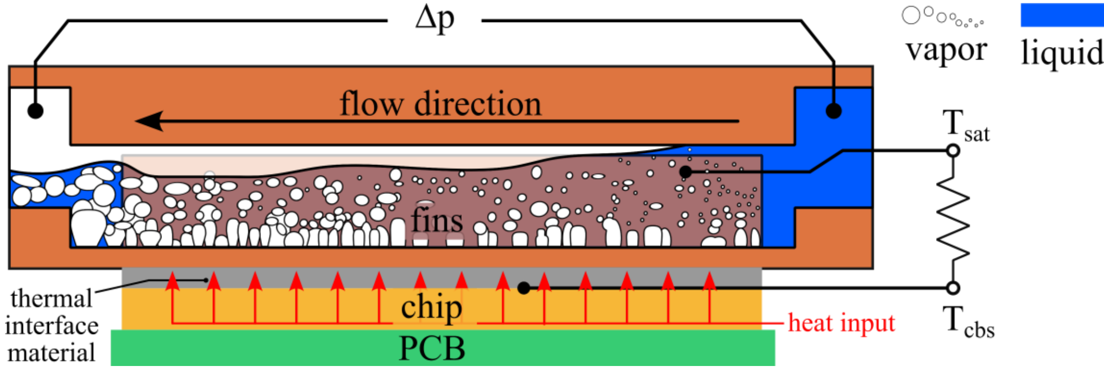

Evaporator test section

Microchannel Flow Lubrication Enhancement

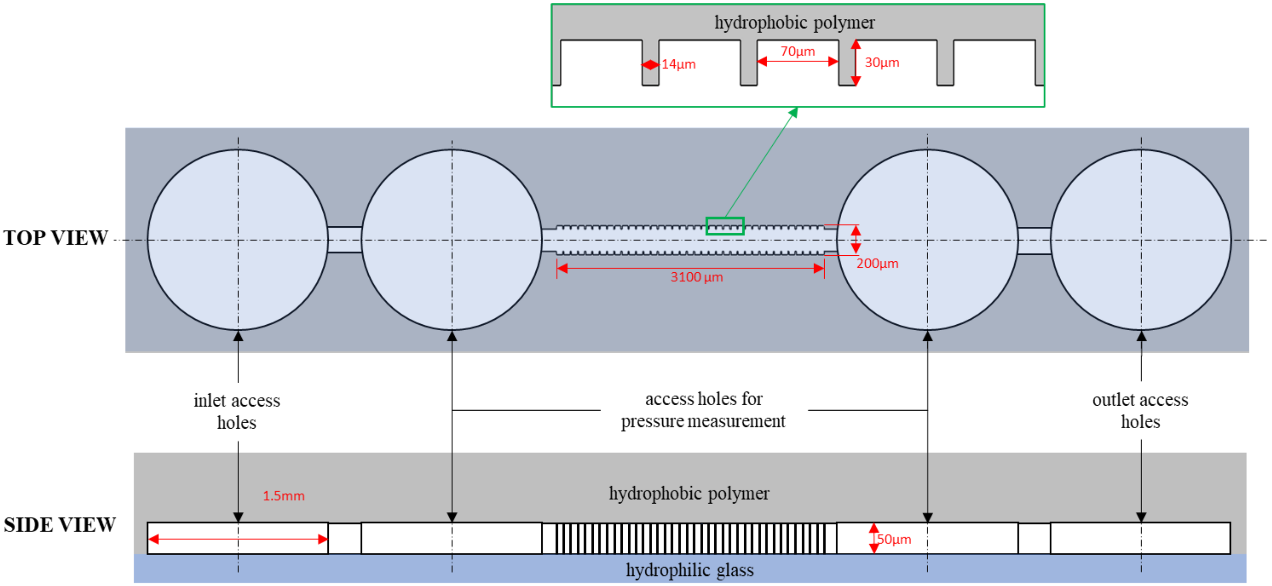

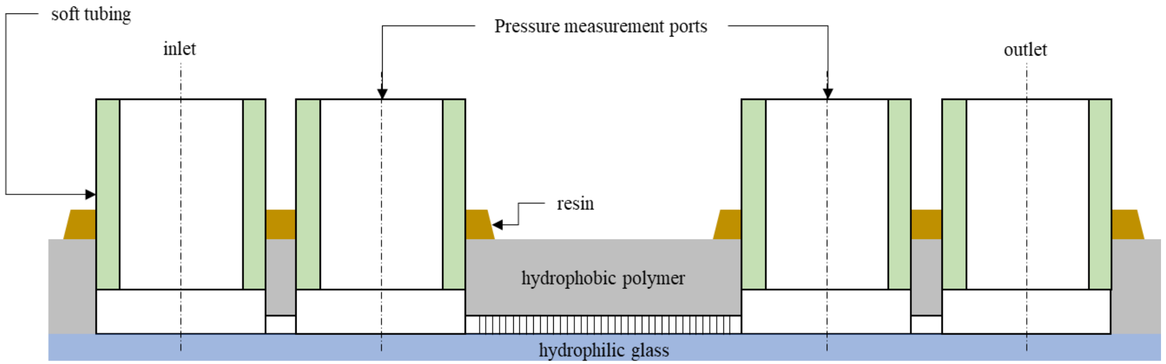

- Microchannel geometry: width 5µm, height 30µm, pitch 25µm
  - Clear meniscus: the surface pattern on side wall allows the easy observation of the shape of the meniscus.
  - Max stability: flow can stay in Cassie state without wetting transition to the Wenzel state.
  - Results verification: verify the measured velocity profile with Byun et al.(2008)

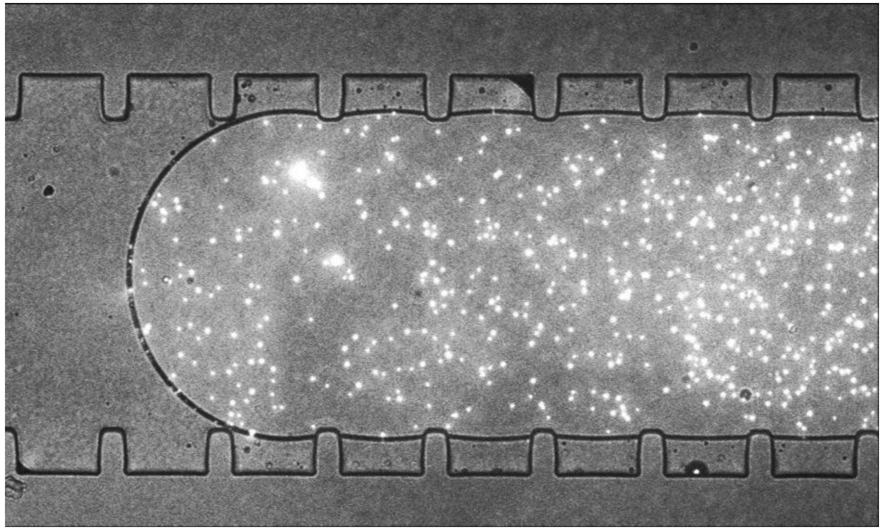

Soft-lithography Process Schematics

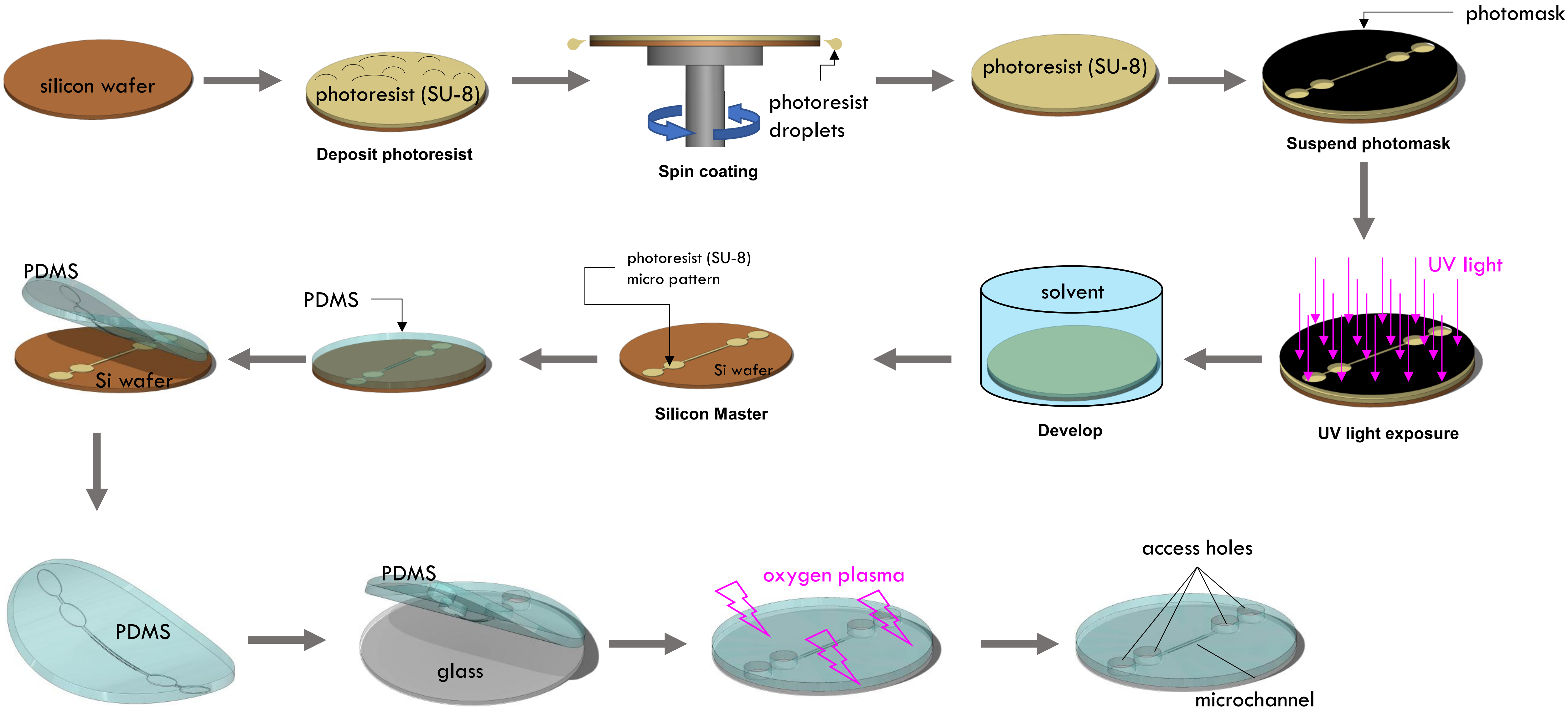

Solution for Cerebral Palsy Patients to Eat Independently